

A New Ceramic–Carbonate Dual-Phase Membrane for High-Flux CO₂ Capture

Shichen Sun, Yeting Wen, and Kevin Huang*

Cite This: *ACS Sustainable Chem. Eng.* 2021, 9, 5454–5460

Read Online

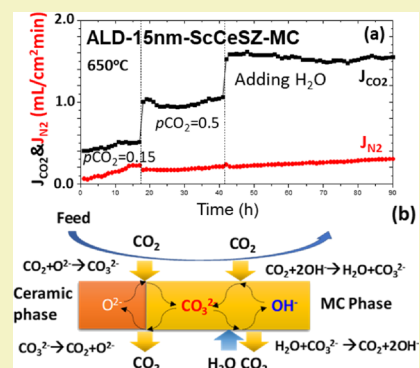
ACCESS |

Metrics & More

Article Recommendations

ABSTRACT: High-temperature membrane-based electrochemical CO₂ capture technology is advantageous in achieving high CO₂ flux without selectivity constraint over its low-temperature counterparts. A high operating temperature also allows *in situ* catalytic conversion of the captured CO₂ into valuable products in the same reactor, thus reducing the overall product cost. Ceramic–carbonate dual-phase membranes are a new class of high-temperature CO₂ capture technology that emerged in recent years, in which the ceramic phase plays a crucial role in the performance. We here report on porous Sc- and Ce-stabilized zirconia (ScCeSZ) as a new ceramic phase in the membrane. The study finds that the wettability between ScCeSZ and molten carbonate (MC) is rather poor, thus requiring surface modification of the ScCeSZ matrix by a wetting agent such as Al₂O₃. The surface-modified ScCeSZ-MC membranes show the highest CO₂ flux density among all ceramic–carbonate dual-phase membranes previously reported, reaching 0.5 and 1.0 mL/cm²/min at 650 °C with 15% CO₂/75% N₂/10% O₂ and 50% CO₂/N₂ as the feed gas, respectively. Long-term testing on the membrane indicates a reasonable flux stability over 200 h. The study also observes that the presence of steam in the sweep gas boosts the CO₂ flux density by 50% without compromising the stability. A mechanism is given to explain the flux enhancement.

KEYWORDS: flux density, stability, surface modification, wettability, leakage



INTRODUCTION

High-temperature CO₂ capture technologies present inherent advantages over low-temperature counterparts because the former can potentially utilize the heat in hot flue gas produced from a combustion process and enable instant conversion of the captured CO₂ into valuable products through catalytic reactions in the same membrane reactors. The recently emerged multiphase solids/molten carbonate (MC)-based CO₂ transporting membranes (CTMs) have been successfully demonstrated in the laboratory to capture CO₂ from CO₂-containing streams such as simulated flue gas at 600–900 °C with high flux and selectivity.^{1–5} The concept of combined CO₂ capture and conversion using CTMs has also been reported for dry (or dry-oxy) reforming of methane into syngas,^{6–10} oxidative dehydrogenation of ethane into ethylene,¹¹ and water-gas shift reaction for H₂ production.¹²

The solid phase in CTMs provides multiple functionalities: a porous matrix to withhold the MC phase, physical support for the membrane, and conductor for oxide ion. The latter is critically important to achieve high CO₂ flux.^{1,10,13–15} For an electron conducting solid, a Ag/MC-based CTM exhibits the highest CO₂ flux because silver possesses a very high electronic conductivity, and the already high ionic conductivity of the MC phase becomes the performance-limiting factor. For an oxide-ion conducting solid, on the other hand, the oxide-ion

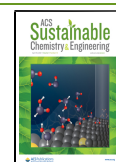
conductivity of the solid phase limits the CO₂ flux due to its lower oxide-ion conductivity than carbonate ion. In other words, to enhance the CO₂ flux of a solid oxide-ion conductor (SOIC)-based CTM, SOICs with high oxide-ion conductivity are highly desirable.

The currently most studied SOICs for CTM applications are CeO₂-based materials.^{12,13,16} Doped CeO₂ SOICs have a reasonably high ionic conductivity under the operating conditions of CTMs, excellent chemical stability, and wettability with MC. For example, Zhang et al. reported a CO₂ flux density as high as 1.84 mL/min/cm² at 700 °C using a 1.2 mm-thick 20% Sm₂O₃-doped CeO₂ (SDC20) as the solid phase.¹² Other materials such as 8 mol % Y₂O₃-doped ZrO₂ (8YSZ) have also been reported, but they generally yield lower CO₂ flux due to its lower oxide-ion conductivity.^{17,18} The well-known Bi₂O₃-based materials with the highest oxide-ion conductivity ever reported did not produce the expected

Received: February 6, 2021

Revised: March 15, 2021

Published: April 8, 2021



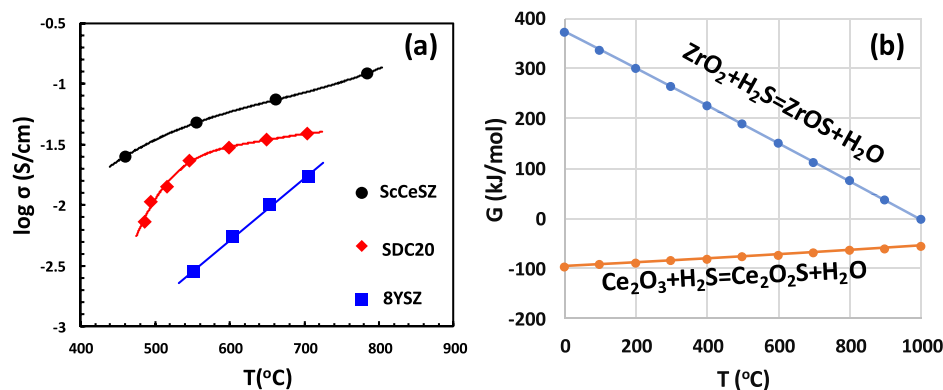


Figure 1. (a) Comparison of oxide-ion conductivity of ScCeSZ, SDC20, and 8YSZ.^{21–23} (b) Gibbs free energy change of the sulfurization reaction on ZrO_2 and Ce_2O_3 .

high CO_2 flux due to their poor chemical stability and inferior wettability with the MC phase.^{4,15}

We here report the use of 10 mol % Sc_2O_3 and 1 mol % CeO_2 -doped ZrO_2 (denoted as ScCeSZ hereinafter)¹⁹ as a SOIC for CTMs with a thickness of 1 mm. The rationale for selecting ScCeSZ is primarily based on its high oxide-ion conductivity, see Figure 1a, which shows ScCeSZ with the highest oxide-ion conductivity when compared to SDC20 and 8YSZ. Another reason for selecting ScCeSZ is that it potentially has a good sulfur tolerance, which is of particular importance to practical application in flue gas that often contains sulfur species such as H_2S . It has been reported that a CeO_2 -based CTM is susceptible to H_2S poisoning by forming Ce_2O_2S .²⁰ Figure 1b compares Gibbs free energy change of the sulfurization reaction on ZrO_2 and Ce_2O_3 (a reduced form of CeO_2 at high temperatures), suggesting that ZrO_2 is unlikely to form $ZrOS$ in H_2S -containing atmospheres. It is also expected that ScCeSZ will have a good chemical compatibility with MC because ZrO_2 -based materials have been previously shown to be stable in MC.^{17,18} What is unknown for ScCeSZ to be a good solid for CTMs is its wettability with MC, which can play a crucial role in MC retention, thus leakage and long-term stability of the CTM. Therefore, in the present study, we focus on investigating the wettability of ScCeSZ with MC, CO_2 flux density, and long-term stability. The measures such as surface modifications leading to improving the wettability between ScCeSZ and MC have been explored. Finally, the effects of partial pressure of CO_2 and H_2O on CO_2 flux density have also been studied using surface-modified ScCeSZ-MC membranes.

EXPERIMENTAL PROCEDURE

Preparation of the ScCeSZ Porous Matrix. The porous ScCeSZ matrix was fabricated by intimately mixing 10 mol % Sc_2O_3 /1 mol % CeO_2 -stabilized ZrO_2 (Sojitz Corporation, denoted as ScCeSZ) powders with carbon black as a pore former in a volume ratio of 3:2 in ethanol. After mixing and drying, the powder mixture was pressed into pellets under ~ 100 MPa followed by sintering at 600 °C for 2 h in air to remove the carbon pore former and 1200 °C for 5 h to achieve good mechanical strength. The dimension of the sintered porous ScCeSZ matrix is ~ 14 mm in diameter and 1 mm in thickness. Its microstructure and microstructural parameters (such as porosity and tortuosity) were examined using a scanning electron microscope (Zeiss Ultra plus FESEM) and a mercury intrusion porosimetry analyzer (AutoPore II, Micromeritics), respectively.

Wettability Study with MC. The wettability of ScCeSZ with MC was also investigated using a dense ScCeSZ pellet. To do so, 0.2 g of eutectic Li–Na (52–48 mol %) carbonate powder was first placed on the top of a dense ScCeSZ pellet followed by heating it to 550, 650,

750, and 850 °C sequentially at a heating rate of 2 °C/min, while physical images of the MC/ScCeSZ couple were taken at each temperature. For comparison, similar MC/solid samples with dense Al_2O_3 and GDC20 ($Gd_{0.2}Ce_{0.8}O_{1.9}$) pellets were also placed next to the MC/ScCeSZ samples for imaging.

Surface Modification of the ScCeSZ Porous Matrix. To enhance the wettability of ScCeSZ with MC, a thin layer of Al_2O_3 was coated over the skeleton of the ScCeSZ porous matrix by an atomic layer deposition (ALD) method. For this process, the porous ScCeSZ matrix was placed inside an ALD reactor chamber (Savannah S200, Cambridge NanoTech, USA). Trimethylaluminum (TMA), DI water, and N_2 were used as the Al_2O_3 precursor, oxidant, and purge/carrier gas, respectively. The reactor chamber temperature was kept at 200 °C. For a typical ALD cycle, the chamber pressure was first decreased to 50 mTorr, and then TMA was introduced into the chamber by a 0.1 s pulse and kept for 20 s to allow it to permeate the porous ScCeSZ matrix. Afterward, N_2 gas was introduced into the chamber to purge out the residual TMA at a flow rate of 20 sccm for 30 s. The chamber was then pumped down to 50 mTorr followed by a 0.015 s pulse of DI water and held for 20 s to fully oxidize the precursor. The deposition rate of the film was determined to be 0.13 nm/cycle by an online QCM (quartz crystal microbalance). The thickness of Al_2O_3 coating was varied in the range of 7 to 26 nm by varying the numbers of deposition cycles from 60 to 200, respectively. After ALD deposition, the samples were calcined at 650 °C for 2 h to ensure the attainment of crystalline Al_2O_3 .

Preparation of ScCeSZ-MC Dual-Phase Membranes. The bare ScCeSZ-MC membranes were prepared by infiltrating *in situ* a eutectic mixture of Li_2CO_3 ($\geq 99\%$, Alfa Aesar) and Na_2CO_3 ($\geq 99\%$, Alfa Aesar) in a molar ratio of 52:48 into the porous ScCeSZ matrix. To do so, the premade carbonate eutectic powder was placed onto the top surface of the ScCeSZ porous matrix, which was sealed onto a supporting Al_2O_3 tube for CO_2 permeation measurement; the details of cell assembling can be found in our previous study.²⁴ For Al_2O_3 surface-modified ScCeSZ-MC membranes, we used an adjusted composition of MC (denoted as adMC) containing Li_2CO_3 : Na_2CO_3 = 57.5:42.5 (mol %) to compensate the loss of Li_2CO_3 due to its reaction with Al_2O_3 forming $LiAlO_2$; the latter has a zero contact angle with MC and is the reason for improving wettability. The eutectic and adjusted MCs were premade by melting them at 510 and 550 °C for 2 h, respectively, followed by grinding them into powders.

CO_2 Flux Measurement. The flux densities of CO_2 of the ScCeSZ-MC membranes fabricated were measured using a home-made permeation cell setup; details on the testing procedure can be found in our previous work.²⁵ For a typical run, a high-purity Ar at a flow rate of 50 mL min^{-1} is used as the sweep gas feeding to one side of the membrane, while a gas mixture (either 75% N_2 /10% O_2 /15% CO_2 or 50% N_2 /50% CO_2) at a flow rate of 100 mL min^{-1} is fed to the other surface as the feed gas. The use of N_2 is also intended to detect any physical leakages from the membrane and gas seals so that the corresponding CO_2 flux correction can be made proportionally.

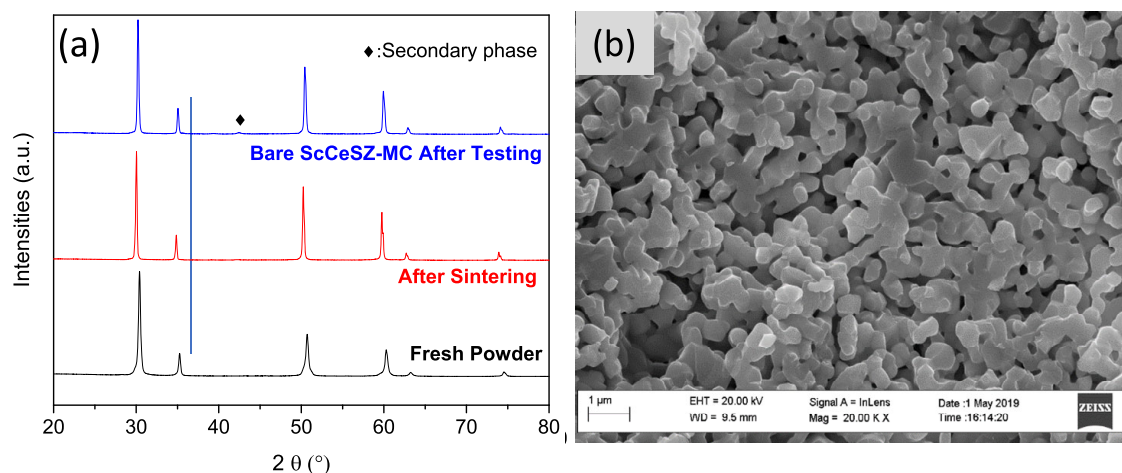


Figure 2. (a) XRD patterns of ScCeSZ at different stages and (b) microstructure of the ScCeSZ porous matrix after sintering at 1200 °C for 5 h.

This is so far the best way that can be used to correct the leakage given the fact that the molecular sizes of CO₂ and N₂ are similar, 3.3 Å for CO₂ vs 3.64 Å for N₂. It is likely that the microstructure such as tortuosity could also play a role in the correction, but it is beyond the scope of this study. The temperature range of the measurement was varied from 550 to 850 °C in a step of 50 °C.

The compositions of the sweep gas were analyzed by an online micro-GC (Agilent Micro GC 490). One hour was given at each temperature to ensure full equilibrium before data were taken. The final CO₂ and N₂ flux densities were calculated using the following equations:

$$J_{\text{CO}_2} = \frac{C_{\text{CO}_2} - C_{\text{Leak}}}{1 - C_{\text{CO}_2} - C_{\text{N}_2} - C_{\text{O}_2}} \times \frac{F_{\text{Ar}}}{A} \quad (1)$$

$$J_{\text{N}_2} = \frac{C_{\text{N}_2}}{1 - C_{\text{CO}_2} - C_{\text{N}_2} - C_{\text{O}_2}} \times \frac{F_{\text{Ar}}}{A} \quad (2)$$

where F_{Ar} is the flow rate of the Ar feed gas, *i.e.*, 50 mL/min; A is the effective area of the membrane, 1.19 cm². To correct the leakage through membrane, the CO₂ flux was adjusted by subtracting C_{Leak} , which equals to $C_{\text{N}_2}/5$ and C_{N_2} for 75% N₂/10% O₂/15% CO₂ and 50% N₂/50% feed gases, respectively.

Other Characterization. The microstructure and compositions of the ScCeSZ matrix, coated or uncoated, along with the final ScCeSZ-MC membranes, before and after testing, were carefully examined by X-ray diffraction (XRD, Rigaku D/MAX-2100 with Cu K α radiation ($\lambda = 1.5418 \text{ \AA}$)) for phase purity and field emission scanning electron microscopy (FESEM, Zeiss Ultra plus) and energy-dispersive spectroscopy (EDS) for uniformity of Al₂O₃ coating and MC distribution. The XRD data were collected from 20° to 80° with an interval of 0.02° and a scan speed of 2° min⁻¹.

RESULTS AND DISCUSSION

Phase Purity and Microstructure of the ScCeSZ Porous Matrix. A pure fluorite cubic structure of ScCeSZ with a lattice parameter of 5.085 Å is confirmed before and after sintering at 1200 °C for 5 h in Figure 2a, which ensures a good oxide-ion conduction. Furthermore, the XRD pattern of the post-tested CTM in Figure 2a also confirms that the phase of ScCeSZ remains largely intact with only a trace of the secondary phase observed. In addition, uniformly distributed pores with a size of <1 μm are observed in Figure 2b for the ScCeSZ porous matrix. The mercury porosimetry measurement reveals that the ScCeSZ matrix possesses a porosity of 34% and an average pore diameter of 0.315 μm.

Wettability of ScCeSZ with MC. Since the wettability of ScCeSZ with MC is important to the retention of MC, thus the stability of membranes, and it is largely unknown in the literature, we performed an experiment of visually observing the shape of MC on a dense ScCeSZ pellet. Figure 3a shows

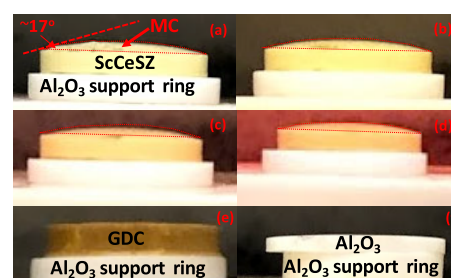


Figure 3. Views of MC (inside dashed circle) on the dense ScCeSZ pellet at (a) 550, (b) 650, (c) 750, and (d) 850 °C; (e) MC on the dense GDC pellet; and (f) MC on the dense Al₂O₃ pellet at 550 °C.

that the MC formed a visible droplet on top of the ScCeSZ pellet at 550 °C and remained so even at higher temperatures. In contrast, the MC flatly run over the GDC and Al₂O₃ dense pellets without any shape maintained at 550 °C. This comparison implies that ScCeSZ has a worse wettability than Al₂O₃ and GDC, which is consistent with a previous study.¹³ Therefore, for ScCeSZ/MC to be a viable membrane, enhancement of wettability is needed.

The consequence of a poor wettability between the porous solid matrix and MC is the loss of MC retention, thus the gas tightness of the membrane. Figure 4a explicitly shows a gradual increase in N₂ leakage with temperature and time of a bare ScCeSZ-MC membrane with a eutectic MC. Such a time-dependent leakage suggests the nature of the porous ScCeSZ matrix gradually losing the retention to MC due to the worsened wettability. At higher temperatures, the viscosity of MC is reduced, further contributing to the loss of MC retention.²⁶ While the N₂ leakage is severe, a high leakage-corrected J_{CO_2} of ~0.6 mL/cm² min is still obtained at 650 °C, which is comparable to that of SDC at 850 °C,¹³ reflecting the potential of ScCeSZ-MC to be a high CO₂ flux membrane if the wettability issue is properly addressed. In addition, it is worth mentioning that a steady state may not have been reached as both J_{CO_2} and J_{N_2} keeps increasing with time as

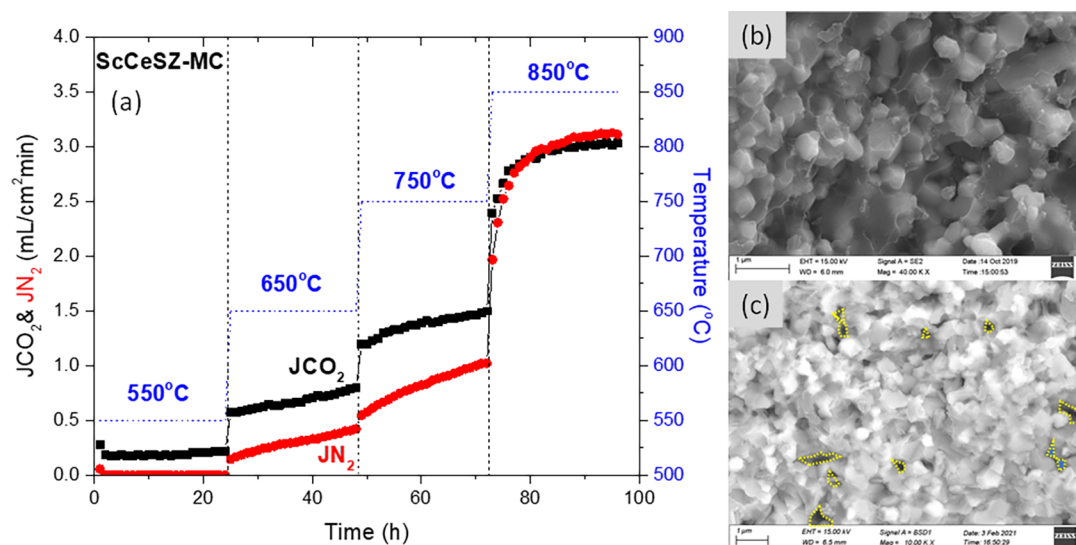


Figure 4. (a) Time-dependent J_{CO_2} and J_{N_2} of a ScCeSZ-MC (eutectic) membrane measured at various temperatures with 50% CO₂ and 50% N₂ feed gas and Ar sweep gas, respectively. SEM images of the cross-sectional microstructure of a bare-ScCeSZ-MC membrane (b) before testing and (c) after testing by back-scattered electron (BSE) imaging, respectively.

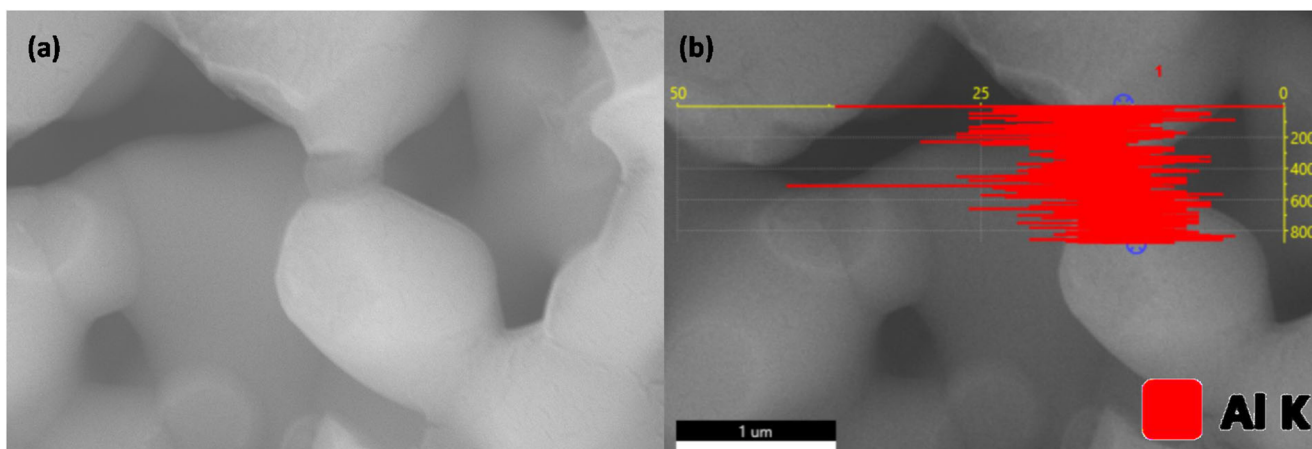


Figure 5. (a) SEM and (b) EDS analysis of Al for the ALD-Al₂O₃-ScCeSZ porous matrix with 7 nm ALD-Al₂O₃.

shown in Figure 4a. We attribute it to the oversimplified N₂ correction for J_{CO_2} (eq 2) mainly based on the fixed CO₂/N₂ ratio in the feed gas, not the microstructure, thus possibly leading to a correction error particularly at high leakage.

The poor wettability of ScCeSZ with MC is further evidenced by the SEM examination. Figure 4b,c shows a cross-sectional view of the bare-ScCeSZ-MC membrane before and after testing, respectively, from which open pores highlighted by yellow dotted lines are visible at both membrane's surface, suggesting that a loss of MC has occurred during testing.

Performance of ALD-Al₂O₃ Surface-Modified ScCeSZ-MC Membranes. The ScCeSZ porous matrix with poor MC wettability was coated with Al₂O₃ in different thicknesses by ALD and evaluated for CO₂ flux. Since it is compositionally difficult to discern Al and Zr by EDS, the latter cannot be used to confirm Al₂O₃ overcoat on the ScCeSZ matrix. A successful deposition of Al₂O₃ on the ScCeSZ matrix is instead confirmed in Figure 5 by SEM imaging and EDS of an Al₂O₃ particle between two ScCeSZ grains. The microstructures of ALD-Al₂O₃-ScCeSZ porous matrices with ALD-Al₂O₃ thicknesses at 7, 15, and 26 nm are shown in Figure 6a-1, b-1, and c-1,

respectively. The EDS analysis indicates that the Al₂O₃ content increases with coating thickness, *i.e.*, ~0.28 wt % for 7 nm, 1.65 wt % for 15 nm, and 2.39 wt % for 26 nm, respectively. Figure 6a-2, b-2, and c-2 shows time- and temperature-dependent J_{CO_2} and J_{N_2} for these membranes. It is evident that, at each temperature, a thicker Al₂O₃ coating reduces N₂ leakage but at a cost of lowered and unstable J_{CO_2} . The SEM images of post-test samples as shown in Figure 6a-3, b-3, and c-3 confirm that the thicker Al₂O₃ coating leads to a denser cross section after testing. It appears that there exists an optimal thickness at 15 nm, where the N₂-leakage rate and J_{CO_2} are balanced. Another trend noticed is that a higher temperature promotes higher N₂ leakage, possibly due to the reduced viscosity of the MC phase. Therefore, it is suggested that surface-modified ScCeSZ-MC membranes should operate below 700 °C to minimize N₂ leakage. Even at lower temperatures, surface-modified ScCeSZ-MC membranes can still yield a high J_{CO_2} (~1.0 mL/cm²·min at 650 °C with 50% CO₂/N₂ feed gas) that is meaningful for practical applications.

Table 1 summarizes the CO₂/N₂ selectivity of ScCeSZ membranes, which indicates a significant improvement in CO₂

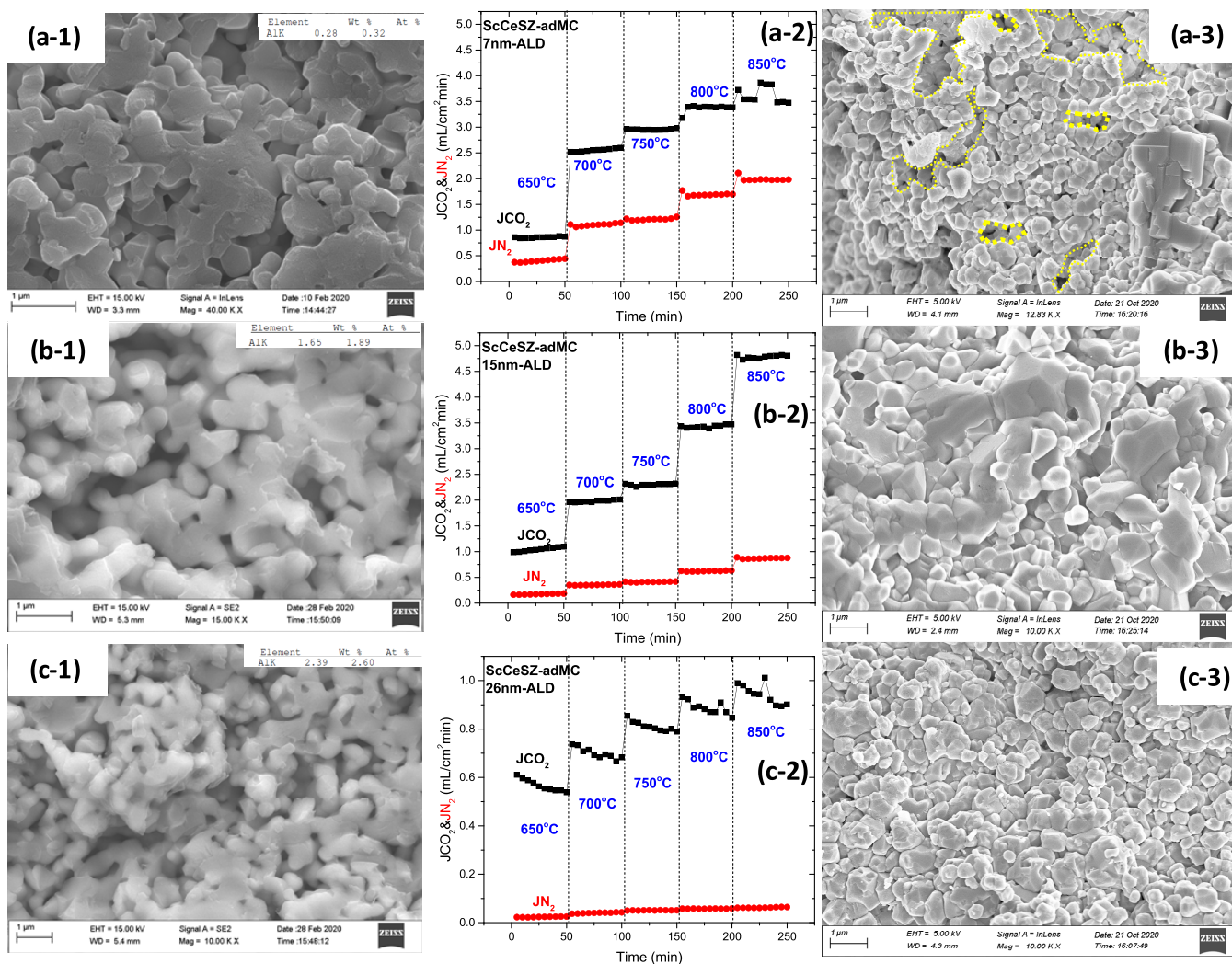


Figure 6. Cross-sectional view and EDS analysis of the ALD- Al_2O_3 -ScCeSZ porous matrix with different ALD- Al_2O_3 thicknesses: (a-1) 7 nm, (b-1) 15 nm, and (c-1) 26 nm before testing and (a-3) 7 nm (some pores were circled inside dashed lines), (b-3) 15 nm, and (c-3) 26 nm after testing; the corresponding flux density vs time for (a-2) 7 nm, (b-2) 15 nm, and (c-2) 26 nm-thick ALD- Al_2O_3 coating. The feed and sweep gas are 50% CO_2 and 50% N_2 and Ar, respectively.

Table 1. CO_2/N_2 Selectivity of ALD- Al_2O_3 -ScCeSZ with 7–26 nm-thick ALD- Al_2O_3 -Coated and Bare ScCeSZ-MC Membranes

T (°C)	7 nm	15 nm	26 nm	bare
650	3.1	7	25.1	3.4
700	3.3	6.6	18.5	
750	3.4	6.6	16.9	2.7
800	3	6.5	16.3	
850	2.8	6.5	16.1	2

selectivity by the ALD- Al_2O_3 coating, especially with increasing Al_2O_3 coating above 7 nm.

A comparison of CO_2 permeability between the ScCeSZ-adMC-modified with 15 nm ALD- Al_2O_3 and those reported in the literature is shown in Figure 7; the test conditions under which these CO_2 fluxes are collected are summarized in Table 2. For a fair comparison, the measured J_{CO_2} shown in Figure 6b-2 is converted into CO_2 permeability as defined by $J_{\text{CO}_2} \cdot L / \Delta p_{\text{CO}_2}$, where Δp_{CO_2} and L are the differential partial pressure of CO_2 across the membrane and thickness of the membrane, respectively. The comparison clearly indicates that

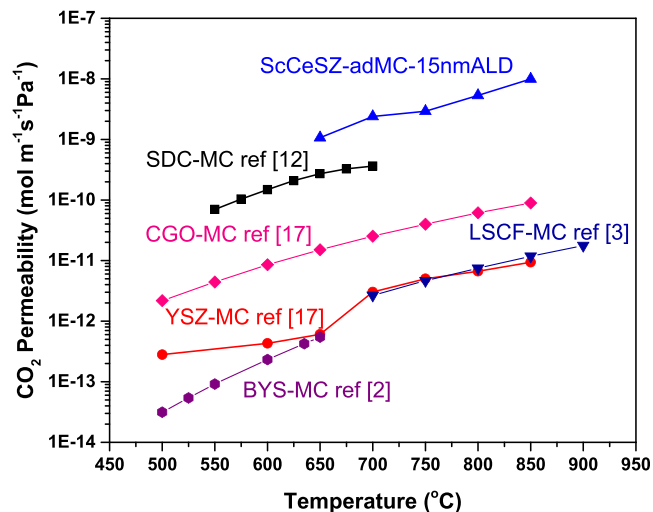


Figure 7. Comparison of CO_2 permeability of ScCeSZ-adMC modified with 15 nm ALD- Al_2O_3 with YSZ-MC and SDC-MC membranes reported in the literature.

Table 2. Conditions under which CO₂ Permeation Flux Is Compared for Three Ceramic–Molten Carbonate Membranes

ceramic phase	membrane thickness (μm)	feed composition	pCO ₂	ref.
Bi _{1.5} Y _{0.3} Sm _{0.2} O _{3-δ} (BYS)	~50	50 mL/min CO ₂ and 50 mL/min Ar	0.5	2
La _{0.6} Sr _{0.4} Co _{0.8} Fe _{0.2} O _{3-δ} (LSCF)	375	50 mL/min CO ₂ and 50 mL/min Ar	0.5	3
Bi _{1.5} Y _{0.3} Sm _{0.2} O _{3-δ} (BYS)	1200	5 mL/min H ₂ , 50 mL/min CO ₂ and 50 mL/min N ₂	0.476	12
Gd _{0.1} Ce _{0.9} O _{2-δ} (CGO)	200–400	7.5 mL/min CO ₂ and 7.5 mL/min He	0.5	17
Y _{0.16} Zr _{0.84} O _{2-δ} (YSZ)	200–400	7.5 mL/min CO ₂ and 7.5 mL/min He	0.5	17
Sc _{0.2} Ce _{0.01} Zr _{0.79} O _{2-δ} (ScCeSZ)	1000	50 mL/min CO ₂ and 50 mL/min Ar	0.5	this work

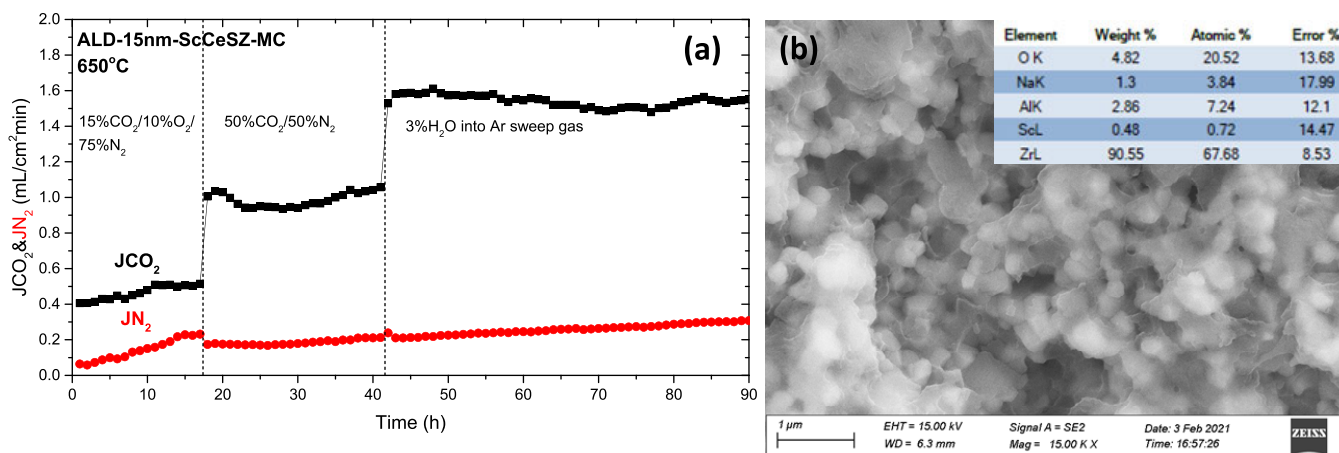


Figure 8. (a) J_{CO_2} and (b) cross-sectional view and EDS analysis of a membrane with 15 nm-thick-ALD- Al_2O_3 -modified ScCeSZ and adMC at 650 °C under two different CO₂ feed gas conditions and 3% H₂O-added sweep gas, respectively.

the permeability of the ScCeSZ-adMC is the highest. The significant improvement in flux is attributed to the high ionic conductivity of ScCeSZ.

The Effect of pCO₂ and pH₂O on J_{CO₂}. The effects of pCO₂ and pH₂O on the J_{CO_2} of ALD-15 nm- Al_2O_3 -ScCeSZ with adMC were further investigated at 650 °C, and the results are shown in Figure 8a. With 15% CO₂/75% N₂/10% O₂ (a mock-up flue gas composition) as the feed gas, J_{CO_2} stabilizes at ~0.5 mL/cm² min after ~20 h. As pCO₂ is increased from 15 to 50% (a mock-up water-gas shift reaction gas composition), the J_{CO_2} increases instantaneously from ~0.5 to ~1.0 mL/cm² min, reflecting that the CO₂ permeation is a chemical potential-driven process. The SEM and EDS analyses in Figure 8b confirm the stability of a membrane with 15 nm-thick-ALD- Al_2O_3 -modified ScCeSZ and adMC after testing.

It is also found that adding H₂O into the sweep side further enhances CO₂ flux density. Figure 8a indicates that adding 3% H₂O into the sweep gas (Ar) can increase J_{CO_2} by ~50% (from ~1.0 to 1.5 mL/cm²/min). It is expected that a higher H₂O content could further enhance J_{CO_2} . During the testing, a relatively low N₂-leakage flux of ~0.2 mL/cm²/min was observed for ~90 h, suggesting that the ALD- Al_2O_3 coating does help the MC retention. The presence of H₂O in the sweep gas did not deteriorate the stability of the membrane. It is worth mentioning that the positive effect of H₂O on the J_{CO_2} of ceramic–carbonate dual-phase membranes has been previously reported by Xing et al.²⁷ This effect is practically important since flue gas always contains a certain level of H₂O. The mechanism behind the flux enhancement is schematically illustrated in Figure 9, where OH[−] is proposed as a product on the sweep side of the membrane, following the reaction below:

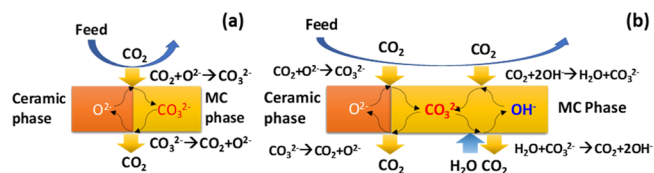


Figure 9. H₂O-enhanced CO₂ transport mechanism in ceramic–carbonate dual-phase membranes under (a) dry and (b) wet conditions.

The generated OH[−] is then transported through the MC phase toward the feed side of the membrane, where it reacts with CO₂ in the feed gas by



The enhanced J_{CO_2} is understood by the fact that the counter diffusion of OH[−] in the MC phase shown in Figure 9b promotes the overall CO₃^{2−} transport by providing an additional CO₃^{2−} transport pathway at the gas/MC two-phase boundaries and through the MC bulk, whereas under dry-gas conditions shown in Figure 9a, CO₃^{2−} transport can only take place at the gas/solid/MC triple-phase boundaries with O^{2−} as the only charge balancing species to CO₃^{2−}.

CONCLUSIONS

In this study, a dual-phase membrane containing MC and high oxide-ion conductivity ScCeSZ has been investigated. The wettability of ScCeSZ is found insufficient to withhold MC for normal CO₂ permeation. The higher the temperature, the worse the MC retention, and thus the higher the N₂ leakage resulted. Surface modification of the ScCeSZ porous matrix by an ALD- Al_2O_3 overcoat with a proper thickness can lead to improved wettability, reduced N₂ leakage, and improved CO₂ flux density; the latter reaches 0.5 and 1.0 mL/cm²/min at 650

°C with 15% CO₂/75% N₂/10% O₂ and 50% CO₂/N₂ as the feed gas, respectively; this level of flux density is significantly higher than those from SDC20 (or other doped CeO₂) and 8YSZ-based ceramic-carbonate dual-phase membranes. Increasing the temperature, *p*CO₂, and *p*H₂O all increase the *J*_{CO₂}, but temperature-increased *J*_{CO₂} is at a cost of increased N₂ leakage. The optimal operating temperature is suggested to be 650 °C, at which the *J*_{CO₂} is still reasonably high. The study also found that introducing 3% H₂O into the sweep gas can enhance the *J*_{CO₂} by 50% without compromising long-term stability.

AUTHOR INFORMATION

Corresponding Author

Kevin Huang – Department of Mechanical Engineering,
University of South Carolina, Columbia, South Carolina
29201, United States;  orcid.org/0000-0002-1232-4593;
Email: huang46@cec.sc.edu

Authors

Shichen Sun – Department of Mechanical Engineering,
University of South Carolina, Columbia, South Carolina
29201, United States

Yeting Wen – Department of Mechanical Engineering,
University of South Carolina, Columbia, South Carolina
29201, United States

Complete contact information is available at:
<https://pubs.acs.org/10.1021/acssuschemeng.1c00860>

Notes

The authors declare no competing financial interest.

ACKNOWLEDGMENTS

We would like to thank the US Department of Energy, Office of Fossil Energy, National Energy Technology Laboratory (award #DE-FE-0031634), and National Science Foundation (award #CBET-1924095) for supporting this work.

REFERENCES

- (1) Xu, N.; Li, X.; Franks, M. A.; Zhao, H.; Huang, K. Silver-molten carbonate composite as a new high-flux membrane for electrochemical separation of CO₂ from flue gas. *J. Membr. Sci.* **2012**, *401-402*, 190–194.
- (2) Rui, Z.; Anderson, M.; Li, Y.; Lin, Y. S. Ionic conducting ceramic and carbonate dual phase membranes for carbon dioxide separation. *J. Membr. Sci.* **2012**, *417-418*, 174–182.
- (3) Anderson, M.; Lin, Y. S. Carbonate-ceramic dual-phase membrane for carbon dioxide separation. *J. Membr. Sci.* **2010**, *357*, 122–129.
- (4) Li, Y.; Rui, Z.; Xia, C.; Anderson, M.; Lin, Y. S. Performance of ionic-conducting ceramic/carbonate composite material as solid oxide fuel cell electrolyte and CO₂ permeation membrane. *Catal. Today* **2009**, *148*, 303–309.
- (5) Chung, S. J.; Park, J. H.; Li, D.; Ida, J.-I.; Kumakiri, I.; Lin, J. Y. S. Dual-phase metal-carbonate membrane for high-temperature carbon dioxide separation. *Ind. Eng. Chem. Res.* **2005**, *44*, 7999–8006.
- (6) Fabián-Anguiano, J. A.; Mendoza-Serrato, C. G.; Gómez-Yáñez, C.; Zeifert, B.; Ma, X.; Ortiz-Landeros, J. Simultaneous CO₂ and O₂ separation coupled to oxy-dry reforming of CH₄ by means of a ceramic-carbonate membrane reactor for in situ syngas production. *Chem. Eng. Sci.* **2019**, *210*, 115250.
- (7) Zhang, P.; Tong, J.; Huang, K. Self-formed, mixed-conducting, triple-phase membrane for efficient CO₂/O₂ capture from flue gas and in situ dry-oxy methane reforming. *ACS Sustainable Chem. Eng.* **2018**, *6*, 14162–14169.
- (8) Michalsky, R.; Neuhaus, D.; Steinfeld, A. Carbon dioxide reforming of methane using an isothermal redox membrane reactor. *Energy Technol.* **2015**, *3*, 784–789.
- (9) Kawi, S.; Kathiraser, Y.; Ni, J.; Oemar, U.; Li, Z.; Saw, E. T. Progress in synthesis of highly active and stable nickel-based catalysts for carbon dioxide reforming of methane. *ChemSusChem* **2015**, *8*, 3556–3575.
- (10) Rui, Z.; Ji, H.; Lin, Y. S. Modeling and analysis of ceramic-carbonate dual-phase membrane reactor for carbon dioxide reforming with methane. *Int. J. Hydrogen Energy* **2011**, *36*, 8292–8300.
- (11) Zhang, P.; Tong, J.; Huang, K. Role of CO₂ in Catalytic Ethane-to-Ethylene Conversion Using a High-Temperature CO₂ Transport Membrane Reactor. *ACS Sustainable Chem. Eng.* **2019**, *7*, 6889–6897.
- (12) Zhang, L.; Xu, N.; Li, X.; Wang, S.; Huang, K.; Harris, W. H.; Chiu, W. K. S. High CO₂ permeation flux enabled by highly interconnected three-dimensional ionic channels in selective CO₂ separation membranes. *Energy Environ. Sci.* **2012**, *5*, 8310–8317.
- (13) Norton, T. T.; Lu, B.; Lin, Y. S. Carbon dioxide permeation properties and stability of samarium-doped-ceria carbonate dual-phase membranes. *J. Membr. Sci.* **2014**, *467*, 244–252.
- (14) Ortiz-Landeros, J.; Norton, T.; Lin, Y. S. Effects of support pore structure on carbon dioxide permeation of ceramic-carbonate dual-phase membranes. *Chem. Eng. Sci.* **2013**, *104*, 891–898.
- (15) Rui, Z.; Anderson, M.; Lin, Y. S.; Li, Y. Modeling and analysis of carbon dioxide permeation through ceramic-carbonate dual-phase membranes. *J. Membr. Sci.* **2009**, *345*, 110–118.
- (16) Patrício, S. G.; Papaioannou, E.; Zhang, G.; Metcalfe, I. S.; Marques, F. M. B. High performance composite CO₂ separation membranes. *J. Membr. Sci.* **2014**, *471*, 211–218.
- (17) Wade, J. L.; Lee, C.; West, A. C.; Lackner, K. S. Composite electrolyte membranes for high temperature CO₂ separation. *J. Membr. Sci.* **2011**, *369*, 20–29.
- (18) Lu, B.; Lin, Y. S. Synthesis and characterization of thin ceramic-carbonate dual-phase membranes for carbon dioxide separation. *J. Membr. Sci.* **2013**, *444*, 402–411.
- (19) Lee, D.-S.; Kim, W. S.; Choi, S. H.; Kim, J.; Lee, H.-W.; Lee, J.-H. Characterization of ZrO₂ co-doped with Sc₂O₃ and CeO₂ electrolyte for the application of intermediate temperature SOFCs. *Solid State Ionics* **2005**, *176*, 33–39.
- (20) Chen, T.; Wu, H.-C.; Li, Y.; Lin, Y. S. Poisoning effect of H₂S on CO₂ permeation of samarium-doped-ceria/carbonate dual-phase membrane. *Ind. Eng. Chem. Res.* **2017**, *56*, 14662–14669.
- (21) Küngas, R.; Vohs, J. M.; Gorte, R. J. Effect of the ionic conductivity of the electrolyte in composite SOFC cathodes. *J. Electrochem. Soc.* **2011**, *158*, B743.
- (22) Xia, C.; Li, Y.; Tian, Y.; Liu, Q.; Zhao, Y.; Jia, L.; Li, Y. A high performance composite ionic conducting electrolyte for intermediate temperature fuel cell and evidence for ternary ionic conduction. *J. Power Sources* **2009**, *188*, 156–162.
- (23) Bodén, A.; Di, J.; Lagergren, C.; Lindbergh, G.; Wang, C. Y. Conductivity of SDC and (Li/Na) 2CO₃ composite electrolytes in reducing and oxidising atmospheres. *J. Power Sources* **2007**, *172*, S20–S29.
- (24) Zhang, P.; Tong, J.; Huang, K. A self-forming dual-phase membrane for high-temperature electrochemical CO₂ capture. *J. Mater. Chem. A* **2017**, *5*, 12769–12773.
- (25) Zhang, P.; Tong, J.; Jee, Y.; Huang, K. Stabilizing a high-temperature electrochemical silver-carbonate CO₂ capture membrane by atomic layer deposition of a ZrO₂ overcoat. *Chem. Commun.* **2016**, *52*, 9817–9820.
- (26) Kojima, T.; Miyazaki, Y.; Nomura, K.; Tanimoto, K. Density, surface tension, and electrical conductivity of ternary molten carbonate system Li₂CO₃–Na₂CO₃–K₂CO₃ and methods for their estimation. *J. Electrochem. Soc.* **2008**, *155*, F150.
- (27) Xing, W.; Peters, T.; Fontaine, M.-L.; Evans, A.; Henriksen, P. P.; Norby, T.; Bredesen, R. Steam-promoted CO₂ flux in dual-phase CO₂ separation membranes. *J. Membr. Sci.* **2015**, *482*, 115–119.